

Automatic Detection of Quiescent Cardiac Phases using Navigator Echoes with Adjacent Complex Correlation Algorithm

M. M. Fung¹, V. B. Ho², M. N. Hood², Y. Zur³, and E. J. Schmidt⁴

¹Applied Science Lab, GE Healthcare, Waukesha, WI, United States, ²Radiology, Uniformed Services University, Bethesda, MD, United States, ³GE Healthcare, Tirat Carmel, Israel, ⁴Radiology, Brigham and Women's Hospital, Boston, MA, United States

PURPOSE

In many cardiac imaging applications, the accurate detection of the systolic and diastolic quiescent periods is critical in obtaining optimal image quality and is usually determined by observing cardiac motion in a CINE acquisition. This complicates the cardiac exam procedure and does not adapt to heart rate variations throughout the exam. In this study, we investigated the feasibility of an automatic detection technique that could detect both cardiac and respiratory motion, and could be adapted to various cardiac sequences.

METHODS

Phantom and volunteer studies were conducted with a 1.5T HDx MRI system with an 8-channel cardiac coil (GE Healthcare, Waukesha, WI). A pencil-beam navigator (in-plane diameter 2cm, 12 turns, 1400 pts, 5.6ms, flip 40°) was used to excite a cylindrical ROI in the left ventricular(LV) free wall in the S/I direction (Fig. 2, blue box). The LV was selected for its high degree of contractility during the cardiac cycle(RR) and its clear interface with the lung, which provides a distinct feature for respiratory motion detection. A flip angle of 40° was used to minimize saturation at the LV when maintaining SNR. After each R peak, a diaphragmic navigator (Fig. 2, green box) was acquired for comparison purposes, and 20 navigator echoes were acquired, at 35ms increments, in each RR (Fig.1). The navigator-echo signal from the channel with the best edge definition was collected for offline analysis in MATLAB (MathWorks, Natick, MA).

The first hypothesis of this study was that the quiescent phases in the RR cycle could be determined by the similarity of one phase with its adjacent phases. We observed that the most quiescent phase had the highest similarity with their adjacent phases, as there was minimal motion between them. Furthermore, the duration of the quiescent period could also be determined by a group of phases that had relatively high similarity with its neighbors. As a result, the following adjacent complex cross correlation algorithm for automatic quiescent phase detection was implemented:

1. Denoising: the navigator echoes were Fourier-transformed, and a 3-pixel median filter was applied to the magnitude and unwrapped-phase data in the image domain to reduce noise
2. For the navigator profile at each cardiac phase i (D_i), the complex cross correlation $CC(i,j)$ with its N nearest neighbors ($j=i-N/2$ to $i+N/2$) was computed (e.q.1), where N depended on the temporal resolution of the navigator echoes ($N = 5$ was used in this study).

$$CC(i, j) = \frac{\sum (D_i - \bar{D}_i) \cdot (D_j - \bar{D}_j)^*}{\sqrt{\sum (D_i - \bar{D}_i)^2 \cdot \sum (D_j - \bar{D}_j)^2}} \quad [1]$$

3. For each phase i , $CC(i,j)$ was summed over its N nearest neighbors.

$$SumCC(i) = \sum_{j=i-N/2}^{j=i+N/2} CC(i, j) \quad [2]$$

4. In each heart cycle, the systolic and diastolic quiet phases were determined as the phase with the maximum $SumCC(i)$ in the first 1/3, and the later 2/3 of the RR, respectively(Fig 3).
5. The duration of the quiet period was determined by applying a threshold T to the $SumCC(i)$ value, about the quiescent phase center, determined in step 4. The duration was defined as the number of phases where $SumCC(i)$ was greater than T . T could be adjusted based on the amount of acceptable motion. In this study, T was defined as 98% of the $SumCC$ distribution range.

A secondary hypothesis of this study was that this data could also be used to detect respiratory motion, as it directly monitored the heart's position. To detect the respiratory motion, we used the systolic frame in the first RR as a reference, and computed the corresponding displacement of the systolic phase in the other RRs using complex cross correlation (eq.1). This process was also repeated for the diastolic phase. This was based on the observation that if the cardiac phases were identical, the shape of the navigator profile would look similar, except for a global shift in position due to respiratory motion. As a result, cardiac and respiratory motion could be decoupled using the above method.

RESULTS

Systolic and diastolic phases in each heart cycle were successfully determined in both phantom and healthy volunteer studies. Figure 4. shows navigator profiles of a volunteer, across multiple RRs. Systolic and diastolic phases and their durations (hollow red & blue boxes, respectively) were detected using the algorithm proposed and matched with the quiescent phases manually observed in the CINE acquisition. The respiratory motions at those phases were also detected (solid red and blue boxes, respectively) and correlated well with the conventional respiratory-navigator-echo collected at the beginning of each RR on the right hemi-diaphragm (green box).

DISCUSSION & CONCLUSION

We have shown the feasibility of automatically detecting cardiac and respiratory motion using navigator echoes

placed at the heart. The use of low flip angle in the pencil beam navigator excitation minimizes LV saturation for the actual image data acquisition. A potential application would be to incorporate this technique into the beginning of various cardiac pulse sequences to collect 2-3 heart beats, determine and then set the appropriate trigger delays and durations for that acquisition automatically. Another application is to prospectively trigger an acquisition based on the cardiac and respiratory state, using real-time filtering[1], and therefore, allowing adaptation to varying heart rate. Furthermore, unlike other self-navigation methods[1,2], where a projection of the excited volume is used and the heart motion is confounded with motion of other structures in the volume, this method acquires the navigator echoes in a localized region directly from the heart. As a result, heart motion was well-isolated, and S/I motion correction could be applied directly to the heart without an assumed relationship with the right hemi-diaphragm[3]. This could improve the robustness and efficiency of cardiac imaging, especially in respiratory-drift situations.

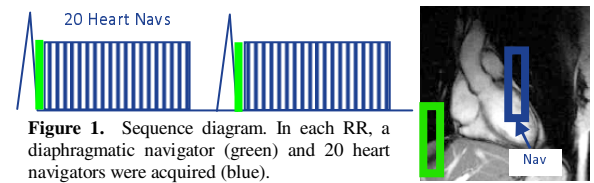


Figure 1. Sequence diagram. In each RR, a diaphragmic navigator (green) and 20 heart navigators were acquired (blue).

Figure 2. Navigator locations

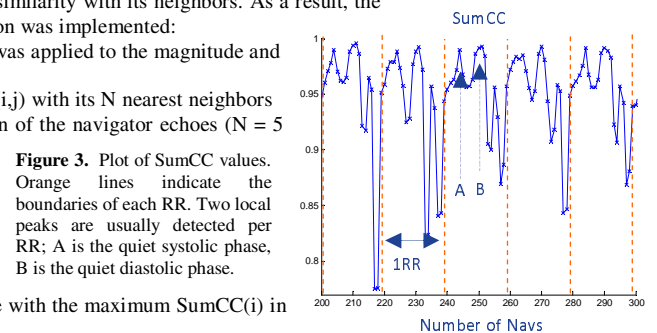


Figure 3. Plot of SumCC values. Orange lines indicate the boundaries of each RR. Two local peaks are usually detected per RR; A is the quiet systolic phase, B is the quiet diastolic phase.

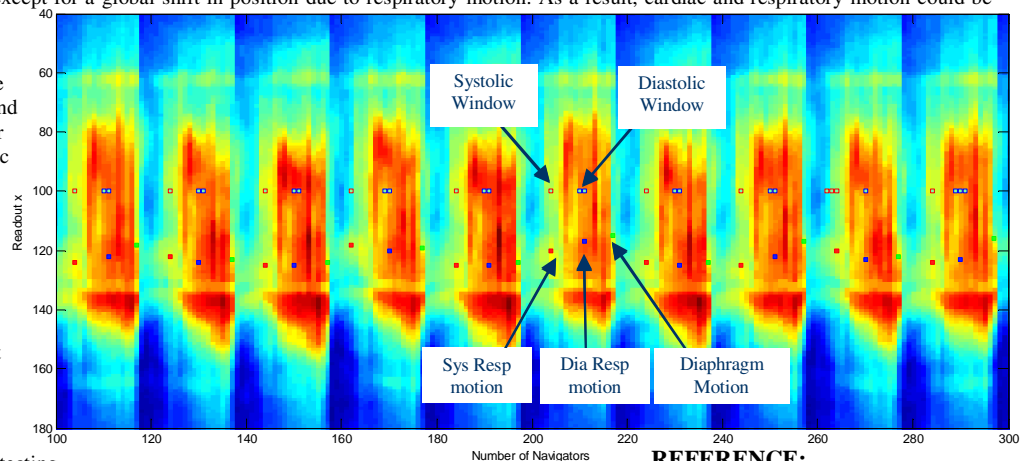


Figure 4. Plot of navigator profile over multiple RRs.

REFERENCE:

- [1] Buehrer, MRM 2008;60:683-690
- [2] Larson AC, MRM 2004; 51:93-102
- [3] Stehning C, MRM 2005; 54: 476-480
- [3] Wang Y, MRM 1995; 33:713-719.